External Synchronization of Solitary States and Chimeras in Unidirectionally Coupled Neural Networks

E. Rybalova, A. Zakharova, and G. Strelkova

Abstract We perform numerical simulation of the dynamics of a multiplex network consisting of two unidirectionally coupled rings of FitzHugh-Nagumo neurons with nonlocal interaction. When uncoupled, one ring demonstrates solitary state regimes and the other one exhibits chimera states. We explore in detail how the synchronization degree between the layers depends on the type of unidirectional interlayer coupling (via fast or slow variables) and on the structures in the driver layer. It is shown that the structure in the response layer can be suppressed and is replaced by the driver layer structure. However, the degree of external synchronization is higher in the case when the driver layer demonstrates solitary states and when the unidirectional coupling is executed via the fast variables. In the case of coupling via the slow variables, external synchronization of neither solitary states nor chimeras cannot be achieved in the considered network.

Keywords Synchronization · FitzHugh-Nagumo neuron · Multiplex network · Chimera state · Solitary state

1 Introduction

Exploring various properties of cooperative dynamics of multicomponent systems, as well as the effects observing in such systems and synchronization between their elements is one of the main part of nonlinear dynamics [1–6]. This is inextricably linked to the fact that most systems in the world are complex networks with various individual elements and types of coupling between them. There is a plenty of works devoted to synchronization phenomena in systems of completely different nature, such as physics [7–10], chemistry [11, 12], neuroscience [13–18], sociologybreak

E. Rybalova (✉) · G. Strelkova
Institute of Physics, Saratov State University, 83 Astrakhanskaya Street, Saratov 410012, Russia
e-mail: rybalovaev@gmail.com

A. Zakharova
Institut für Theoretische Physik, Technische Universität Berlin, Hardenbergstr. 36, 10623 Berlin, Germany

C. H. Skiadas and Y. Dimotikalis (eds.), *14th Chaotic Modeling and Simulation International Conference*, Springer Proceedings in Complexity,
https://doi.org/10.1007/978-3-030-96964-6_26

[19–21], etc., as well as in real-world systems, for instance, communication systems [22], power grids [23, 24], transportation networks [25].

Dynamics of ensembles of nonlocally coupled elements, when each node is coupled with a finite number of its nearest neighbors, has recently attracted much interest due to the discovery of a new spatiotemporal structure, later called "chimera state" [26, 27]. This structure is a striking example of cluster synchronization when a network dynamics spontaneously splits into coherent (synchronous behavior) and incoherent (desynchronized dynamics) clusters with well-defined boundaries in the network space. Although these structures have been found in networks with different individual elements [26–32], with different types of coupling between them [28, 33–37], as well as in real experiments [7–11, 38, 39], greater interest in these structures was caused by their connection with natural and man-made dynamics [14, 17, 22–25].

Solitary states are another example of partial synchronization [40]. With this type of synchronization, solitary nodes appear on the coherent profile of the system and are evenly distributed over the entire ensemble. Oscillators in the solitary state regime fundamentally differ in their dynamics from the other oscillators of the network. This kind of pattern has been observed in networks of the Kuramoto models [40–42], the discrete-time systems [43], the FitzHugh-Nagumo systems [44–46], and others. They have also been detected in experiments with mechanical pendulums [39]. Later, solitary state chimeras were revealed when an incoherent cluster includes several solitary states and coexists with coherent clusters [46, 47].

Studying interaction between different spatiotemporal structures is an important task in the numerical simulation of collective dynamics of complex systems. It was shown in [30] that chimera states can be observed in a ring of nonlocally coupled FitzHugh-Nagumo oscillators. Later, these studies were expanded in [46] and it was found out that this network can also demonstrate solitary states. The interaction between chimeras and solitary states was explored for the first time in [48] where two rings of nonlocally coupled FitzHugh-Nagumo oscillators were bidirectionally coupled either via fast or slow variables. The objective of the present paper is to study the peculiarities of external synchronization of chimeras and solitary states in a two-layer network of unidirectionally coupled rings of FitzHugh-Nagumo oscillators depending on the type of interlayer coupling (via activators or inhibitors) and of the spatiotemporal structures in a driver and a response layer. The identity of synchronous structures in the considered network is quantified using a global interlayer synchronization error.

2 Model Under Study

The model under study represents a multiplex network consisting of two unidirectionally coupled layers. Each layer is given by a ring of nonlocally coupled FitzHugh-Nagumo oscillators [49, 50]. The network is governed by the following system of equations:

$$\begin{aligned}
\varepsilon \frac{du_{1i}}{dt} &= u_{1i} - \frac{u_{1i}^3}{3} - v_{1i} + \frac{\sigma}{2P} \sum_{j=i-P}^{i+P} [b_{uu}(u_{1j} - u_{1i}) + b_{uv}(v_{1j} - v_{1i})] + c^u(u_{2i} - u_{1i}), \\
\frac{dv_{1i}}{dt} &= u_{1i} + a + \frac{\sigma}{2P} \sum_{j=i-P}^{i+P} [b_{vu}(u_{1j} - u_{1i}) + b_{vv}(v_{1j} - v_{1i})] + c^v(v_{2i} - v_{1i}), \\
\varepsilon \frac{du_{2i}}{dt} &= u_{2i} - \frac{u_{2i}^3}{3} - v_{2i} + \frac{\sigma}{2P} \sum_{j=i-P}^{i+P} [b_{uu}(u_{2j} - u_{2i}) + b_{uv}(v_{2j} - v_{2i})] + s^u(u_{1i} - u_{2i}), \\
\frac{dv_{2i}}{dt} &= u_{2i} + a + \frac{\sigma}{2P} \sum_{j=i-P}^{i+P} [b_{vu}(u_{2j} - u_{2i}) + b_{vv}(v_{2j} - v_{2i})] + s^v(v_{1i} - v_{2i}).
\end{aligned} \tag{1}$$

Dynamical variables u_{li} correspond to the activators or the fast variables, and v_{li} are the inhibitors or the slow variables in each ring, where $l = 1, 2$ is the layer number, and $i = 1, 2, \ldots, N = 300$ is the node number in each ring (all indices are modulo N). Individual FitzHugh-Nagumo oscillators can demonstrate either excitable ($|a| > 1$) or oscillatory ($|a| < 1$) regimes, which depend on the excitability threshold parameter a. In the present study, all the FitzHugh-Nagumo oscillators in the network (1) operate in the oscillatory regime at $a = 0.5$ and the time-scale separation parameter is also fixed $\varepsilon = 0.05$ for all the network nodes.

The nonlocal intralayer coupling in each layer is given by the coupling strength σ and the coupling range P which denotes the number of nearest neighbors of the ith node from both sides in each layer. In our numerical simulation we choose $\sigma = 0.3$ and $P = 105$ in both rings. The intralayer interaction of the FitzHugh-Nagumo neurons in the system (1) has not only direct couplings between activator (u) and inhibitor (v) variables but also cross ones which are executed according to a rotational coupling matrix:

$$B = \begin{pmatrix} b_{uu} & b_{uv} \\ b_{vu} & b_{vv} \end{pmatrix} = \begin{pmatrix} \cos\phi & \sin\phi \\ -\sin\phi & \cos\phi \end{pmatrix}, \tag{2}$$

where $\phi \in [-\pi; \pi)$. In the work [30] this type of coupling was used for the first time and it has been shown that chimera states can be observed in the ring of nonlocally coupled FitzHugh-Nagumo neurons at $\phi = \pi/2 - 0.1$. This research was expanded in the paper [46] where the effect of parameter ϕ on the regimes observed in the FitzHugh-Nagumo ring was explored in detail. It was particularly shown that this ensemble can demonstrate not only chimera states but also solitary states. In the present research the parameter ϕ_l ($l = 1, 2$) values are set in such a way to observe a solitary state regime in the first ring and chimera states in the second one.

The interlayer coupling in the network (1) is organized to be unidirectional with coefficients c^u, c^v, s^u, and s^v. Therefore, when the first layer affects the second one (solitary states affect chimeras) we have $c^u = 0$, $c^v = 0$, $s^u \neq 0$, $s^v \neq 0$, where the superscripts correspond to the coupling via the fast (u) or the slow (v) variables. Vice versa, when the first layer is subjected to the second one (chimeras affect

solitary states), the interlayer coupling is defined by $c^u \neq 0, c^v \neq 0, s^u = 0, s^v = 0$. In our simulations, initial conditions are chosen to be randomly distributed on circle $u^2 + v^2 \leqslant 2^2$. The layers are coupled from the initial time $t = 0$, and the equations (1) are integrated using the Runge-Kutta-Fehlberg method with step $h = 0.02$.

Figure 1 shows typical spatiotemporal structures which can be observed in uncoupled FitzHugh-Nagumo rings for the chosen intralayer coupling parameter values. The first layer demonstrates the solitary states (Fig. 1a–c), and the second layer exhibits the chimera state (Fig. 1d–f). As can be seen from Fig. 1a, the solitary nodes are evenly distributed along the coherent profile, while the mean phase velocity profile is rather flat (Fig. 1b) (this parameter is calculated with the formula $\omega_{li} = \frac{2\pi M_i}{\Delta T}$, where M_i is the number of complete rotations around the origin performed by the ith oscillator during the time interval ΔT [30], $l = 1, 2$ is the layer number). Differences in the dynamics of the solitary nodes and the oscillators from the coherent part can be observed in the (u_1, v_1) phase plane (Fig. 1c), where the attracting set with a large radius (black dots) corresponds to the oscillators from the coherent region, and the small cycle (red dots) to the solitary nodes. In the case of chimera states, the snapshot of the second ring dynamics splits into two clusters (Fig. 1d): one includes elements $150 \leqslant i \leqslant 250$ with coherent dynamics, and the other one consists of nodes $1 \leqslant i \leqslant 149$ and $251 \leqslant i \leqslant 300$ which behave incoherently. In the mean phase velocity profile (Fig. 1e), the coherent domain is characterized by a smooth distribution, while an arc-like dependence is characteristic for the nodes from the incoherent cluster. There are also two intersecting sets in the (u_2, v_2) phase plane (Fig. 1f): the green attractor reflects the dynamics of the elements from the incoherent cluster of the chimera state and the black set refers to the nodes from the coherent domain. As can be seen from the phase portraits, the green attracting set is essentially thick if compared with a limit cycle for a single FitzHugh-Nagumo system [49, 50], and unlike the solitary states, these sets are overlapping.

To analyze the degree of synchronous behavior (or identity of synchronous structures) of the coupled layers we apply a global interlayer synchronization error:

$$\delta = \frac{1}{N} \sum_{i=1}^{N} \left(\frac{1}{t_2 - t_1} \int_{t_1}^{t_2} (u_{1i} - u_{2i})^2 dt \right), \tag{3}$$

where $N = 300$. Since the coupled FitzHugh-Nagumo rings (1) are not identical, the external interlayer synchronization can be considered in its effective sense. In our numerical studies, imposing certain quantitative conditions for the global interlayer synchronization error we can distinguish effective external synchronization if $0.001 < \delta < 0.01$ and full (complete) external synchronization when $\delta < 0.001$.

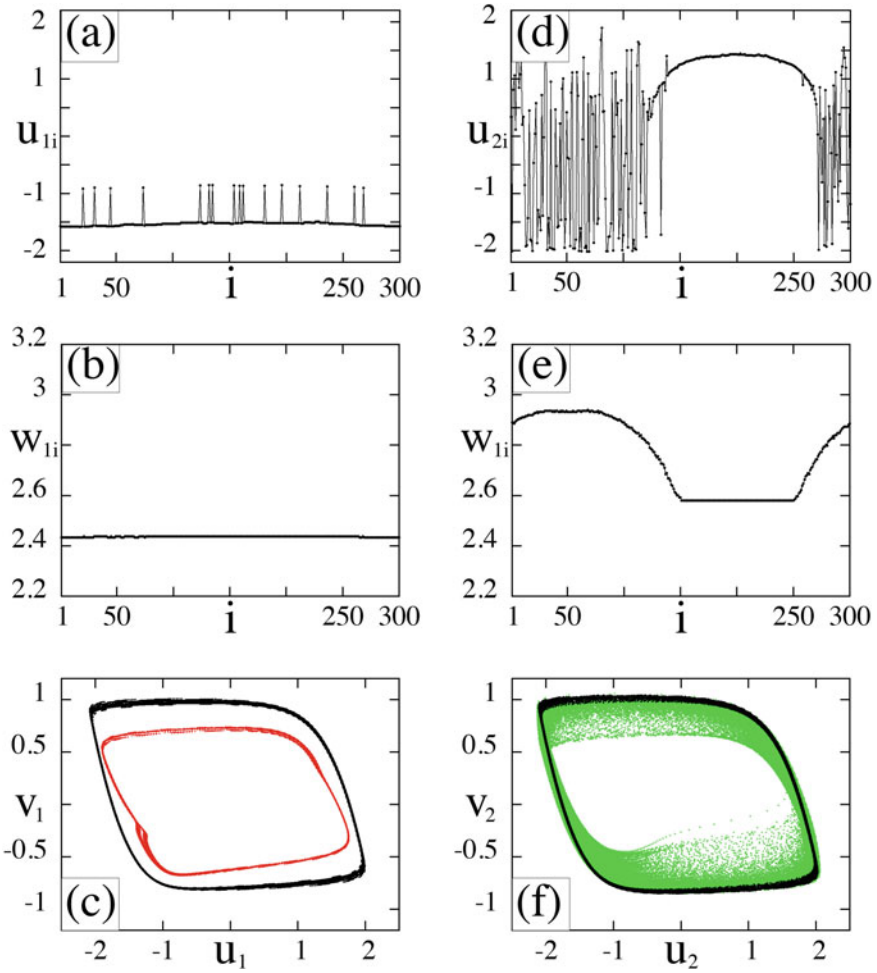

Fig. 1 Dynamics of uncoupled rings ($c^u = 0, c^v = 0, s^u = 0, s^v = 0$): the solitary states in the first ring (**a**–**c**) and the chimera state in the second ring (**d**–**f**). Snapshots of variables u_{1i} and u_{2i} (upper row), mean phase velocity profiles (middle row, ω_{1i}, ω_{2i}) and phase portraits for all elements of the rings (lower row, (u_1, v_1) and (u_2, v_2)). Black lines on the phase portraits correspond to elements in the coherent mode, red curves to the solitary nodes, and green ones to the incoherent cluster of the chimera state. Parameters: $\sigma = 0.3$, $P = 105$, $\phi_1 = \pi/2 - 0.2$, $\phi_2 = \pi/2 - 0.04$, $\varepsilon = 0.05$, $a = 0.5$, and $N = 300$

3 Unidirectional Interlayer Coupling via Fast Variables

We study numerically the case when the FitzHugh-Nagumo rings (1) are unidirectionally coupled via the fast variables, i.e., $c^u \neq 0$, $s^u \neq 0$ and $c^v = 0$, $s^v = 0$. It was shown in [48] that in the presence of this type of the interlayer coupling in a system of two symmetrically coupled rings, first chimera states are formed in both rings, then with an increase in the coupling strength, the rings are completely synchronized and their dynamics correspond to coherent spatial profiles. However, at certain values of the interlayer coupling strength, the regime of solitary states can also be observed in both rings.

3.1 Impact of Solitary States on Chimera

Let us first consider the possibility of suppressing the chimera structure in the second ring and the establishment of solitary states under the unidirectional influence of the first ring which demonstrates the solitary states. In this case the first FitzHugh-Nagumo ring is a driver ($c^u = 0, c^v = 0$), while the second one is a response ($s^u \neq 0$, $s^v = 0$). Figure 2 illustrates the dependence of the global interlayer synchronization error and the evolution of the second ring dynamics when the interlayer coupling strength s^u grows. As can see from Fig. 2b, already for a sufficiently weak coupling, the chimera state in the second ring completely disappears and is replaced by the regime of solitary states. However, the observed structure is not synchronous with that one in the driver (see Figs. 1a and 2b): the frequency of the solitary nodes is not equal to that of the elements from the coherent part of the ring (Fig. 2c), and the corresponding attracting set (red points) in the phase plane (inset in Fig. 2c) is wider than that shown in Fig. 1c. As follows from Fig. 2a, when the interlayer coupling is sufficiently weak ($s^u < 0.15$), the synchronization error δ does not satisfy the effective synchronization condition.

Even when s^u slightly increases, the observed solitary state regime in the second ring is still not synchronous to the mode in the first ring (Fig. 2d and e). However, as can be seen from the phase portrait in Fig. 2e, the set corresponding to the solitary nodes (red points) is separated from the oscillators from the coherent profile (black line). Starting from the region where the dependence $\delta(s^u)$ becomes smooth ($s^u > 0.33$ in Fig. 2a), the solitary nodes in the second ring begin to correspond to the solitary nodes in the first ring (Fig. 1c). In this case we have a smooth frequency profile and two phase portraits clearly separated in the phase space (Fig. 2f and g). On the other hand, already starting from $s^u > [0.15; 0.28]$ (the exact value depends on the initial conditions) the global interlayer synchronization error becomes less than 0.01 and we can talk about effective synchronization. Only when $s^u > 0.67$ (Fig. 2a), complete external synchronization ($\delta < 0.001$) occurs in the network (1).

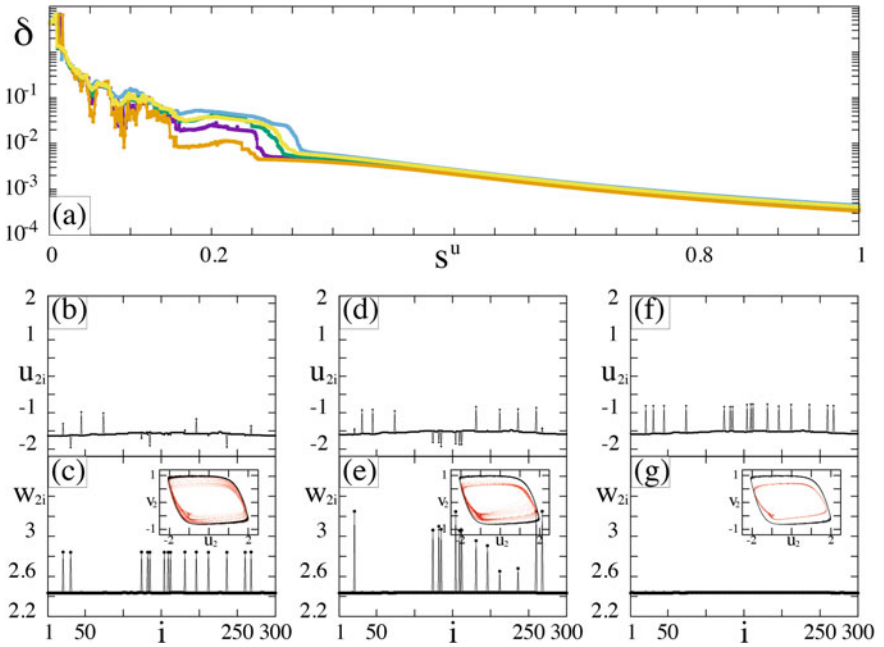

Fig. 2 Unidirectional impact of the first ring (solitary states) on the second one (chimera) via the fast variables: $s^u \neq 0$, $s^v = 0$, $c^u = 0$, $c^v = 0$ in the network (1). **a** Dependence of δ (3) on the interlayer coupling strength s^u plotted for 5 different sets of random initial conditions in each ring (marked by different colors). **b**–**g** Dynamics of the second ring for increasing s^u: 0.035 (**b**, **c**), 0.13 (**d**, **e**), 0.35 (**f**, **g**). **b**, **d**, **f** Snapshots of variables u_{2i}, **c**, **e**, **g** mean phase velocity profiles w_{2i} and phase portraits for all ring elements (insets (u_2, v_2)): black lines indicate the coherent dynamics, red curves correspond to the solitary nodes. Other parameters: $\sigma = 0.3$, $P = 105$, $\phi_1 = \pi/2 - 0.2$, $\phi_2 = \pi/2 - 0.04$, $\varepsilon = 0.05$, $a = 0.5$, and $N = 300$

3.2 *Impact of Chimera on Solitary States*

When the second ring exhibiting the chimera state is the driver, the global synchronization error δ demonstrates a smooth dependence on the interlayer coupling strength c^u over the entire interval of its variation (Fig. 3a). This can be explained by the fact that there is no need to synchronize individual elements (solitary nodes) which introduce deviations into dependence $\delta(c^u)$. In this case, the solitary states in the first ring also quickly disappear, and the snapshot splits into coherent and incoherent clusters (Fig. 3c). However, the arc-like dependence does not immediately appear on the frequency profile (Fig. 3c). Increasing c^u leads to the appearance of the arc in the frequency profile, which at first looks a bit noisy (Fig. 3e). Only when c^u grows ($c^u > 0.1$), the frequency profile becomes smooth (Fig. 3g). As follows from the snapshots (Fig. 3d and f) and the phase portraits (insets in Fig. 3e and g), already at a very weak interlayer coupling c^u, the first ring (response) starts behaving similarly to the second ring (driver) (see Figs. 1d, f and 3d, e).

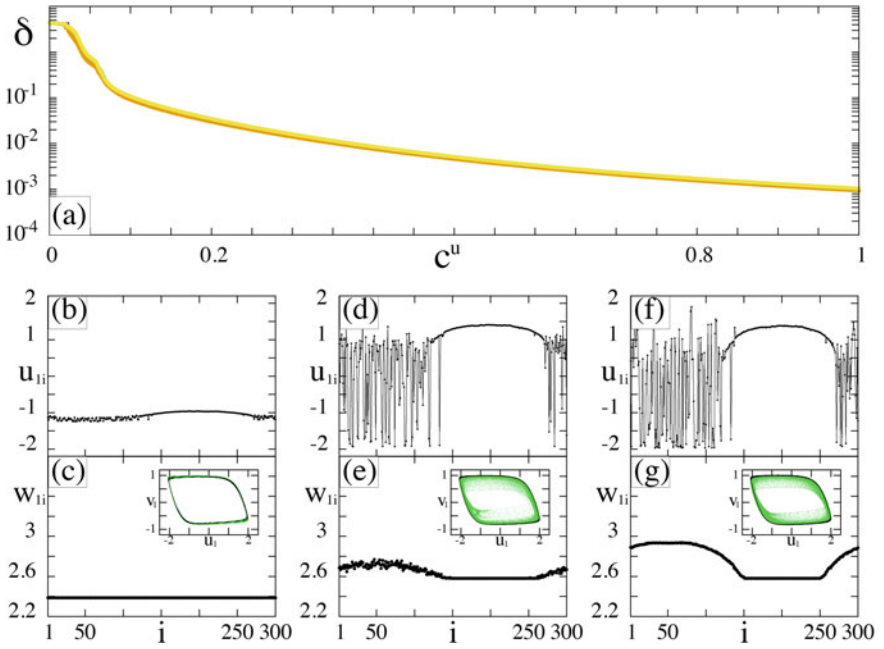

Fig. 3 Unidirectional impact of the second ring (chimera) on the first ring (solitary states) via the fast variables: $c^u \neq 0$, $s^u = 0$, $s^v = 0$, $c^v = 0$ in the network (1). **a** Dependence of δ (3) on the interlayer coupling strength c^u plotted for 5 different sets of random initial conditions in each ring (marked by different colors). **b**–**g** Dynamics of the first ring in (1) for increasing c^u: 0.014 (**b**, **c**), 0.06 (**d**, **c**), 0.235 (**f**, **g**). **b**, **d**, **f** Snapshots of variables u_{1i}, **c**, **e**, **g** mean phase velocity profiles w_{1i} and phase portraits for all ring elements (insets (u_1, v_1)): black lines indicate the coherent dynamics, red curves correspond to the solitary nodes. Other parameters are as in Fig. 2

In contrast to the previously considered case, in this situation the global interlayer synchronization error does not fall below the 0.001 level even for a rather strong unidirectional interlayer coupling (Fig. 3a). This means that only effective external synchronization of the chimera state takes place.

4 Unidirectional Interlayer Coupling via Slow Variables

We now turn to the case when the two rings (1) are unidirectionally coupled via the slow variables, i.e., $c^v \neq 0$, $s^v \neq 0$, while there is no coupling via the fast variables, $c^u = 0$, $s^u = 0$. Our previous studies [48] showed that with this type of coupling in a system of two bidirectionally coupled rings, firstly the chimera states in the second ring disappear and are replaced by uniformly distributed solitary nodes, but they are not synchronous with the solitary nodes in the first ring. At the same time, the solitary nodes in the first ring gradually disappear. A further increase of the coupling

strength between the layers leads to a coherent regime in the first ring and the solitary state chimera in the second ring. By increasing the coupling strength, we can observe the classical chimera states in both rings, which behave quite synchronously. With a further increase in the coupling strength the dynamics of the two-layer network is similar to the dynamics of the rings which are coupled through the fast variables. The rings are completely synchronized and their behavior corresponds to coherent spatial profiles. Moreover, at certain values of the interlayer coupling strength (more than 1.0), the solitary state mode can be observed in both rings.

4.1 Impact of Solitary States on Chimera

Consider the case when the second ring in the chimera state is driven via the slow variables by the first ring in the solitary state regime. In this case the chimera state also quickly disappears and is replaced by the solitary nodes (Fig. 4b–e). However, the solitary nodes are distributed throughout the whole ring and their location does not coincide with that in the driver layer (see Figs. 1a and 4d). It is also evident that the frequencies of several solitary nodes are not equal to the frequency of the other oscillators, as it should be (Fig. 4e). Moreover, in the phase portrait, the trajectories of some solitary nodes do not lie separately from the phase portrait of the oscillators from the coherent domain, i.e., there is an intersection of the red and black sets (inset in Fig. 4e). When the interlayer coupling increases, the most part of the solitary nodes disappears but the remaining nodes are not synchronized with those in the first ring (Fig. 4f and g). A further increase in s^v does not lead to the observation of a more synchronous mode of oscillations of the second ring with the first one, but, on the contrary, leads to the fact that the phase portraits of the elements change greatly and the rings are never synchronized (for example, Fig. 5).

Let us pay attention to the change in the global interlayer synchronization error δ as s^v increases (Fig. 4a). Within the interval $s^v \in [0; 0.2]$, the dependence has several minima and maxima and does not smoothly decrease when s^v grows. This is due to the fact that initially, under the influence of the first ring, the chimera state in the second ring is gradually destroyed (the first minimum is at $s^v \approx 0.04$). Then a lot of solitary nodes appear in the second ring, which do not correspond to the solitary nodes in the first ring and are not synchronized with them (maximum is at $s^v \approx 0.055$) (see Figs. 1a and 4d). Afterwards, the solitary nodes gradually disappear with increasing coupling strength (minimum is at $s^v \approx 0.11$). Finally, the solitary nodes in the second ring correspond to the same oscillators as in the first ring (maximum is at $s^v \approx 0.2$) (see Figs. 1a and 4f), and the rings are partially synchronized with a further increase of the coupling strength s^v. However, even for a rather strong coupling strength s^v, even effective external synchronization is not observed in the network (1) since $\delta > 0.01$.

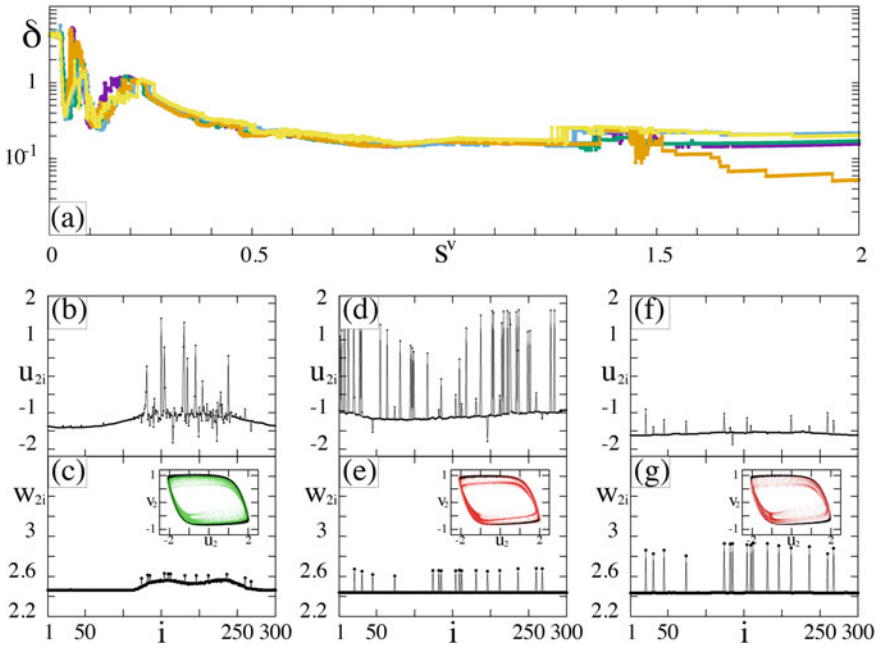

Fig. 4 Numerical results for the case when the first ring (solitary states) is unidirectionally coupled with the second one (chimera state) via the slow variables: $s^v \neq 0$, $s^u = 0$, $c^u = 0$, $c^v = 0$. **a** Dependence of δ (3) on the interlayer coupling strength s^v plotted for 5 different sets of random initial conditions in each ring (marked by different colors). **b**–**g** Dynamics of the second ring for increasing s^v: 0.025 (**b**, **c**), 0.062 (**d**, **c**), 0.5 (**f**, **g**). **b**, **d**, **f** Snapshots of variables u_{2i}, **c**, **e**, **g** mean phase velocity profiles w_{2i} and phase portraits for all ring elements (insets (u_2, v_2)): black lines indicate the coherent dynamics, red curves correspond to the solitary nodes. Other parameters: $\sigma = 0.3$, $P = 105$, $\phi_1 = \pi/2 - 0.2$, $\phi_2 = \pi/2 - 0.04$, $\varepsilon = 0.05$, $a = 0.5$, and $N = 300$

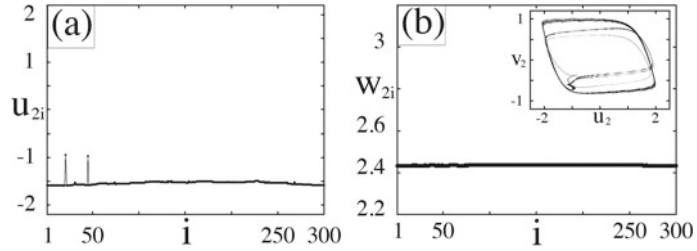

Fig. 5 Dynamics of the second ring under the unidirectional impact from the first ring at $s^v = 1.446$ ($s^u = 0, c^u = 0, c^v = 0$). **a** Snapshots of variables u_{2i}, **b** mean phase velocity profiles w_{2i} and phase portraits for all ring elements (insets (u_2, v_2)): black lines indicate the coherent dynamics, red curves correspond to the solitary nodes. Other parameters are as in Fig. 4

4.2 Impact of Chimera on Solitary States

Finally, we explore the network (1) dynamics when the driver layer (the second ring) exhibits the chimera state. In this case, the network dynamics is similar to that which is observed when the unidirectional coupling is executed via the fast variables. The solitary nodes in the first ring gradually disappear as the coupling strength c^v increases (Fig. 6b and c), and the snapshots of the first ring dynamics (Fig. 6d and e) consist of incoherent and coherent parts, that is related to the chimera state. However, even with a strong coupling, in the presence of a well-developed chimera state in the first layer, the frequency profile demonstrates only a barely noticeable arc-like structure (Fig. 6f and g). Synchronization between the rings is not achieved even for a very strong interlayer coupling: the global interlayer synchronization error never goes below 0.1 (see Fig. 6a). However, for certain sets of random initial conditions in each ring, the values of δ can be lower than for the other sets (see the blue line in Fig. 6a).

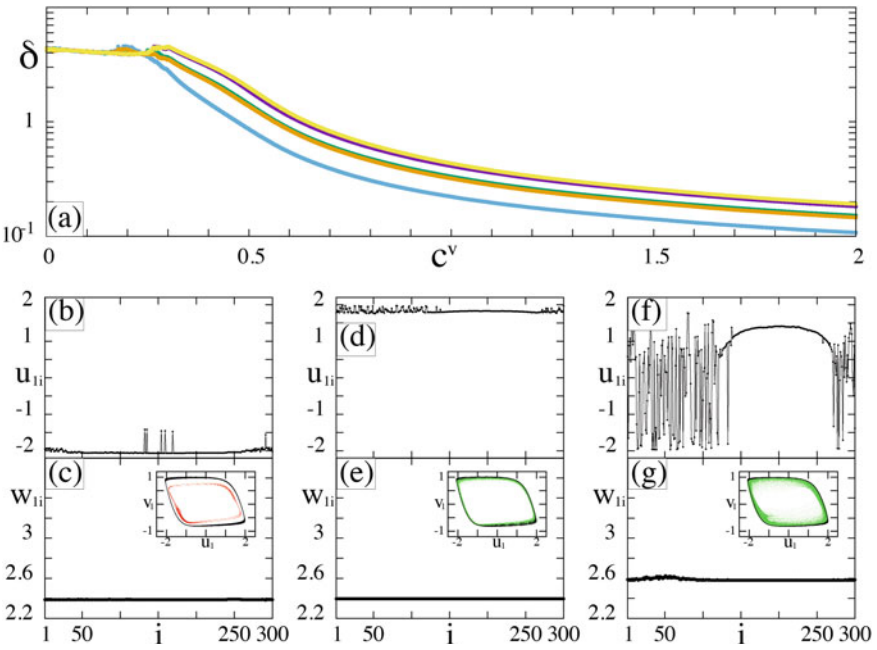

Fig. 6 Numerical results for the case when the first ring (solitary states) in the network (1) is driven by the second ring (chimera) via the slow variables: $c^v \neq 0, s^v = 0, s^u = 0, c^u = 0$. **a** Dependence of δ (3) on the interlayer coupling strength c^u plotted for 5 different sets of random initial conditions in each ring (marked by different colors). **b–g** Dynamics of the first ring in (1) for increasing c^v: 0.025 (**b**, **c**), 0.223 (**d**, **c**), 1.6 (**f**, **g**). **b**, **d**, **f** Snapshots of variables u_{1i}, **c**, **e**, **g** mean phase velocity profiles w_{1i} and phase portraits for all ring elements (insets (u_1, v_1)): black lines indicate the coherent dynamics, red curves correspond to the solitary nodes. Other parameters are as in Fig. 4

5 Conclusion

In this paper we have presented results of numerical simulation of a two-layer multiplex network of unidirectionally coupled rings of FitzHugh-Nagumo oscillators. Our studies have shown that in the case of unidirectional coupling via the fast variables (activators), it is possible to suppress both chimera states and solitary states and establish a different spatiotemporal regime. However, with external synchronization of solitary states, the global interlayer synchronization error shows a stronger similarity between the rings than in the case of synchronization of chimera states. This fact is easily explained by the structure of these states. Since the oscillators in the coherent cluster are synchronized more easily, it is natural to assume that the solitary states will demonstrate a higher degree of synchronization.

In the case of unidirectional coupling between the FitzHugh-Nagumo rings via the slow variables (inhibitors), although the initial structure of the ring is rapidly destroyed under external influence, the structure of the driver layer can be only partially reproduced in the response layer. This fact is confirmed by the global interlayer synchronization error which does not fall below 0.01.

Thus, our studies have shown that both solitary states and chimera states can be suppressed when the two layers are unidirectionally coupled via both the fast and the slow variables. The response layer reproduces the structure of the driver layer instead of its own. However, the effect of external synchronization (both effective and complete) is observed only when the layers are coupled via the activators. These studies can be useful in practical applications when it is needed to suppress one of the structures and establish another one. Thus, one can control the dynamics of multilayer networks.

Acknowledgements This work was supported by the Deutsche Forschungsgemeinschaft (DFG, German Research Foundation)-Projektnummer 163436311-SFB 910 and by the RFBR and the DFG according to the Research Project No. 20-52-12004.

References

1. V.S. Afraimovich, V.I. Nekorkin, G.V. Osipov, V.D. Shalfeev. *Stability, Structures and Chaos in Nonlinear Synchronization Networks* (World Scientific, 1995)
2. V.N. Belykh, I.V. Belykh, E. Mosekilde, Cluster synchronization modes in an ensemble of coupled chaotic oscillators. Phys. Rev. E **63**(3), 036216 (2001)
3. V. Nekorkin, M.G. Velarde, *Synergetic Phenomena in Active Lattices: Patterns, Waves, Solitons, Chaos* (Springer, 2002)
4. G.V. Osipov, J. Kurths, Ch. Zhou, *Synchronization in Oscillatory Networks* (Springer, 2007)
5. V.I. Nekorkin, A.S. Dmitrichev, D.V. Kasatkin, V.S. Afraimovich, Relating the sequential dynamics of excitatory neural networks to synaptic cellular automata. Chaos **21**(4), 043124 (2011)
6. S. Boccaletti, A.N. Pisarchik, C.I. Del Genio, A. Amann, *Synchronization: From Coupled Systems to Complex Networks* (Cambridge University Press, 2018)
7. A.M. Hagerstrom, T.E. Murphy, R. Roy, P. Hövel, I. Omelchenko, E. Schöll, Experimental observation of chimeras in coupled-map lattices. Nat. Phys. **8**(9), 658–661 (2012)

8. F. Rogister, R. Roy, Localized excitations in arrays of synchronized laser oscillators. Phys. Rev. Lett. **98**(10), 104101 (2007)
9. M. Wickramasinghe, I.Z. Kiss, Spatially organized partial synchronization through the chimera mechanism in a network of electrochemical reactions. Phys. Chem. Chem. Phys. **16**(34), 18360–18369 (2014)
10. D.P. Rosin, D. Rontani, N.D. Haynes, E. Schöll, D.J. Gauthier, Transient scaling and resurgence of chimera states in networks of Boolean phase oscillators. Phys. Rev. E **90**(3), 030902 (2014)
11. M.R. Tinsley, S. Nkomo, K. Showalter, Chimera and phase-cluster states in populations of coupled chemical oscillators. Nat. Phys. **8**(9), 662–665 (2012)
12. J.F. Totz, J. Rode, M.R. Tinsley, K. Showalter, H. Engel, Spiral wave chimera states in large populations of coupled chemical oscillators. Nat. Phys. **14**(3), 282–285 (2018)
13. A.E. Pereda, Electrical synapses and their functional interactions with chemical synapses. Nat. Rev. Neurosci. **15**(4), 250–263 (2014)
14. T. Chouzouris, I. Omelchenko, A. Zakharova, J. Hlinka, P. Jiruska, E. Schöll, Chimera states in brain networks: empirical neural vs. modular fractal connectivity. Chaos **28**(4), 045112 (2018)
15. P.J. Uhlhaas, W. Singer, Neural synchrony in brain disorders: relevance for cognitive dysfunctions and pathophysiology. Neuron **52**(1), 155–168 (2006)
16. P. Jiruska, M. De Curtis, J.G. Jefferys, C.A. Schevon, S.J. Schiff, K. Schindler, Synchronization and desynchronization in epilepsy: controversies and hypotheses. J. Physiol. **591**(4), 787–797 (2013)
17. R.G. Andrzejak, C. Rummel, F. Mormann, K. Schindler, All together now: analogies between chimera state collapses and epileptic seizures. Sci. Rep. **6**(1), 1–10 (2016)
18. C. Hammond, H. Bergman, P. Brown, Pathological synchronization in Parkinson's disease: networks, models and treatments. Trends Neurosci. **30**(7), 357–364 (2007)
19. M. Girvan, M.E. Newman, Community structure in social and biological networks. Proc. Natl. Acad. Sci. **99**(12), 7821–7826 (2002)
20. R. Amato, A. Díaz-Guilera, K.K. Kleineberg, Interplay between social influence and competitive strategical games in multiplex networks. Sci. Rep. **7**(1), 1–8 (2017)
21. R. Amato, N.E. Kouvaris, M. San Miguel, A. Díaz-Guilera, Opinion competition dynamics on multiplex networks. N. J. Phys. **19**(12), 123019 (2017)
22. S. Hong, Y. Chun, Efficiency and stability in a model of wireless communication networks. Social Choice Welfare **34**(3), 441–454 (2010)
23. P.J. Menck, J. Heitzig, J. Kurths, H.J. Schellnhuber, How dead ends undermine power grid stability. Nat. Commun. **5**(1), 1–8 (2014)
24. B. Wang, H. Suzuki, K. Aihara, Enhancing synchronization stability in a multi-area power grid. Sci. Rep. **6**(1), 1–11 (2016)
25. A. Cardillo, M. Zanin, J. Gómez-Gardenes, M. Romance, A.J. del Amo, S. Boccaletti, Modeling the multi-layer nature of the European Air Transport Network: resilience and passengers re-scheduling under random failures. Eur. Phys. J. Spec. Topics **215**(1), 23–33 (2013)
26. Y. Kuramoto, D. Battogtokh, Coexistence of coherence and incoherence in nonlocally coupled phase oscillators. Nonlinear Phenom. Complex Syst. **5**(4), 380–385 (2002)
27. D.M. Abrams, S.H. Strogatz, Chimera states for coupled oscillators. Phys. Rev. Lett. **93**(17), 174102 (2004)
28. I. Omelchenk, Y. Maistrenko, P. Hövel, E. Schöll, Loss of coherence in dynamical networks: spatial chaos and chimera states. Phys. Rev. Lett. **106**(23), 234102 (2011)
29. M.J. Panaggio, D.M. Abrams, Chimera states: coexistence of coherence and incoherence in networks of coupled oscillators. Nonlinearity **28**(3), R67 (2015)
30. I. Omelchenko, E. Omelchenko, P. Hövel, E. Schöll, When nonlocal coupling between oscillators becomes stronger: patched synchrony or multichimera states. Phys. Rev. Lett. **110**(22), 224101 (2013)
31. A. Zakharova, M. Kapeller, E. Schöll, Chimera death: symmetry breaking in dynamical networks. Phys. Rev. Lett. **112**(15), 154101 (2014)
32. S.A. Bogomolov, A.V. Slepnev, G.I. Strelkova, E. Schöll, V.S. Anishchenko, Mechanisms of appearance of amplitude and phase chimera states in ensembles of nonlocally coupled chaotic systems. Commun. Nonlinear Sci. Numer. Simul. **43**, 25–36 (2017)

33. S. Ulonska, I. Omelchenko, A. Zakharova, E. Schöll, Chimera states in networks of Van der Pol oscillators with hierarchical connectivities. Chaos **26**(9), 094825 (2016)
34. E. Schöll, Synchronization patterns and chimera states in complex networks: interplay of topology and dynamics. Eur. Phys. J. Spec. Topics **225**(6), 891–919 (2016)
35. J. Sawicki, I. Omelchenko, A. Zakharova, E. Schöll, Chimera states in complex networks: interplay of fractal topology and delay. Eur. Phys. J. Spec. Topics **226**(9), 1883–1892 (2017)
36. S.I. Shima, Y. Kuramoto, Rotating spiral waves with phase-randomized core in nonlocally coupled oscillators. Phys. Rev. E **69**(3), 036213 (2004)
37. M.J. Panaggio, D.M. Abrams, Chimera states on a flat torus. Phys. Rev. Lett. **110**(9), 094102 (2013)
38. E.A. Martens, S. Thutupalli, A. Fourriere, O. Hallatschek, Chimera states in mechanical oscillator networks. Proc. Natl. Acad. Sci. **110**(26), 10563–10567 (2013)
39. T. Kapitaniak, P. Kuzma, J. Wojewoda, K. Czolczynski, Y. Maistrenko, Imperfect chimera states for coupled pendula. Sci. Rep. **4**, 6379 (2014)
40. Y. Maistrenko, B. Penkovsky, M. Rosenblum, Solitary state at the edge of synchrony in ensembles with attractive and repulsive interactions. Phys. Rev. E **89**(6), 060901 (2014)
41. H. Wu, M. Dhamala, Dynamics of Kuramoto oscillators with time-delayed positive and negative couplings. Phys. Rev. E **98**(3), 032221 (2018)
42. P. Jaros, S. Brezetsky, R. Levchenko, D. Dudkowski, T. Kapitaniak, Y. Maistrenko, Solitary states for coupled oscillators with inertia. Chaos **28**(1), 011103 (2018)
43. E. Rybalova, N. Semenova, G. Strelkova, V. Anishchenko, Transition from complete synchronization to spatio-temporal chaos in coupled chaotic systems with nonhyperbolic and hyperbolic attractors. Eur. Phys. J. Spec. Topics **226**(9), 1857–1866 (2017)
44. L. Schülen, D.A. Janzen, E.S. Medeiros, A. Zakharova, Solitary states in multiplex neural networks: onset and vulnerability. Chaos Solitons Fractals **145**, 110670 (2021)
45. L. Schülen, S. Ghosh, A.D. Kachhvah, A. Zakharova, S. Jalan, Delay engineered solitary states in complex networks. Chaos Solitons Fractals **128**, 290–296 (2019)
46. E. Rybalova, V.S. Anishchenko, G.I. Strelkova, A. Zakharova, Solitary states and solitary state chimera in neural networks. Chaos **29**(7), 071106 (2019)
47. A. Bukh, E. Rybalova, N. Semenova, G. Strelkova, V. Anishchenko, New type of chimera and mutual synchronization of spatiotemporal structures in two coupled ensembles of nonlocally interacting chaotic maps. Chaos **27**(11), 111102 (2017)
48. E.V. Rybalova, A. Zakharova, G.I. Strelkova, Interplay between solitary states and chimeras in multiplex neural networks. Chaos Solitons Fractals **148**, 111011 (2021)
49. R. FitzHugh, Impulses and physiological states in theoretical models of nerve membrane. Biophys. J. **1**(6), 2061–2070 (1961)
50. J. Nagumo, S. Arimoto, S. Yoshizawa, An active pulse transmission line simulating nerve axon. Proc. IRE **50**(10), 2061–2070 (1962)